URSI AP-RASC, Sydney, Australia, 17 – 22 August 2025

Instantaneous Frequency Measurement using Single Sideband Modulation of Mach-Zehnder Modulators

Qingchuan Huang [(1)], Tetsuya Kawanishi [(1)]
(1) Department of Electronic and Physical Systems, Graduate School of Fundamental Science and Engineering, Waseda University, Tokyo, Japan, e-mail: hqcgearing@akane.waseda.jp

Abstract

Autonomous driving technology relies on in-vehicle radar, which plays a crucial role in detecting surrounding objects. However, in environments with multiple radars, radio interference can degrade radar performance. This paper proposes a real-time frequency measurement method based on single sideband (SSB) modulation, requiring only two instantaneous sideband values for accurate measurement. The feasibility and accuracy of the proposed method were experimentally demonstrated.

1. Introduction

In recent years, the telecommunication systems have become the foundation of modern society and continue to evolve in rapid speed. The fifth-generation mobile communication system (5G) provide higher-speed and larger-capacity transmission compared with former 4G network, overcoming the existed problem in 4G network such as limitations in communication speed and latency. With such kind of advantages such as high bandwidth, low latency, high reliability, and massive connectivity, 5G and the next generation Beyond 5G, is expected to contribute to the future IoT society [1].

One of the key technologies expected to play an active role in future IoT society is autonomous driving. In-vehicle radar is an essential component of autonomous driving, enabling object detection in place of human perception. As autonomous driving systems become more widespread, the use of automotive radar is expected to increase significantly. Under such conditions, the detection performance of in-vehicle radar may degrade due to radio interference, potentially compromising the safety of autonomous driving [2]. To mitigate this issue, a technology capable of instantly measuring the frequency bands of signals used around vehicles is required.

In this study, we propose an instantaneous frequency measurement method that uses the single sideband modulation of the Mach-Zehnder modulator (MZM). By individually adjusting the bias state of sub MZM, the hole dual-parallel Mach-Zehnder modulator (DPMZM) can be set as the single sideband modulation state. In this method, the sweep RF signals are feeding to dual-parallel Mach-Zehnder modulator, inducing the sideband change in the optical spectrum. The optical output was converted into electrical signal using the PD because the traditional optical spectrum analysis requires a longer sweeping time. The phase measurement results can be derived from the ratio of the 1st order and -1st order sidebands, meaning the measurement of two data points. Moreover, the measurement method was experimentally demonstrated under millimeter wave band, and the calculation in the electrical signal domain was conducted using two different configurations: the analog division circuit and the field-programmable gate array (FPGA).

2. Theory

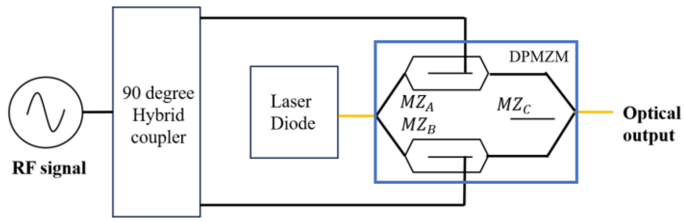

Figure 1. Configuration of optical SSB modulation

The optical single sideband modulation can be realized by adjusting the bias voltage of a dual-parallel Mach-Zehnder modulator [3]. When a phase difference exists, an imbalance occurs between the intensities of the upper sideband (USB) and lower sideband (LSB) [4]. By adjusting for the bias, it is possible to eliminate one sideband component (USB or LSB). The configuration of SSB modulation using the DPMZM is shown in Figure 1. The DPMZM comprises three sub-MZMs: MZ_A, MZ_B, and MZ_C. The procedure for SSB modulation is as follows. First, MZ_A and MZ_B are set to null bias to suppress the carrier component. The MZ_C are adjusted to quadrature bias to suppress the intensity of one sideband (USB or LSB) while maximizing the intensity of the other [5]. A 90 degree phase difference is induced by the 90 degree hybrid coupler between the modulation signals input to MZ_A and MZ_B. The modulation signals exerted on MZ_A and MZ_B can be expressed as follows.

$$v_A(t) = A_m cos\omega_m t \quad (1)$$

$$v_B(t) = A_m sin\omega_m t \quad (2)$$

The optical outputs from MZ_A and MZ_B can be expressed as.

$$R_A = \frac{1}{2\sqrt{2}}\left[e^{i(\omega_0 t + A_m cos\omega_m t)} - e^{i(\omega_0 t - A_m cos\omega_m t)}\right] \quad (3)$$

$$R_B = \frac{1}{2\sqrt{2}}\left[e^{i(\omega_0 t + A_m sin\omega_m t)} - e^{i(\omega_0 t - A_m sin\omega_m t)}\right] \quad (4)$$

If the phase variation with the voltage applied to MZ_C is denoted as $f(t)$, the output light can be expressed as:

$$R = \frac{1}{\sqrt{2}}\left[R_A \times e^{if(t)} + R_B \times e^{-if(t)}\right] \quad (5)$$

Ignoring the influence of the third or higher order sideband components, the optical output can be expressed as:

$$R = e^{i\left[\omega_0 t + \frac{\pi}{4}\right]}[\cos[f(t) + \pi/4]J_1(A_m)e^{i\omega_m t} + isin\left[f(t) + \frac{\pi}{4}\right]J_1(A_m)e^{-i\omega_m t}] \quad (6)$$

From (6), it can be understood that by varying the voltage applied to MZ_C and adjusting the $f(t)$ to $\pm\pi/4$, it is possible to realize the selection of LSB or USB.

When we add the phase difference of -Φ(t) to the modulation signal, the expression of the modulation signals $v_A(t)$ and $v_B(t)$ can be written as:

$$v_A(t) = A_m \cos(\omega_m t) \quad (7)$$

$$v_B(t) = A_m \cos\{\omega_m t - (\Phi(t) - \frac{\pi}{2})\} \quad (8)$$

Refer to (3), (4) and (6), and set $f(t)$ as $\pm\pi/4$ to satisfy the requirement of SSB modulation. Then, the optical output can be expressed in the form of Bessel functions.

$$R = \frac{i}{2}e^{i\omega_0 t + \frac{\pi}{4}}J_1(A_m)\left[e^{i\omega_m t}\{1 + e^{-i\Phi(t)}\} + e^{-i\omega_m t}\{1 + e^{i(\Phi(t) - \pi)}\}\right] \quad (9)$$

According to (9), the sideband component with an angular frequency $\omega_0 + n\omega_n$ has the amplitude $J_1(A_m)\{1 + e^{-i\Phi(t)}\}/2$. The power of the of 1st and -1st order sideband components P_1 and P_{-1} can be expressed as:

$$P_1 = \frac{{J_1}^2(A_m)}{2}(1 + cos\Phi(t)) \quad (10)$$

$$P_{-1} = \frac{{J_1}^2(A_m)}{2}(1 - cos\Phi(t)) \quad (11)$$

Equations (10) and (11) describe the relationship between the sideband components and the phase difference. However, the amplitude of the input optical signal and the transmittance of the phase modulator are not considered and it is inappropriate to derive the phase difference from either (10) or (11). Therefore, the appropriate phase difference should be derived from the ratio of P_1 to P_{-1}, which can be written as:

$$\frac{P_{-1}}{P_1} = \frac{1 - cos\Phi(t)}{1 + cos\Phi(t)}$$

$$= \frac{1 - \left(1 - 2sin^2\frac{\Phi(t)}{2}\right)}{1 + \left(2cos^2\frac{\Phi(t)}{2} - 1\right)} \quad (12)$$

$$= \frac{sin^2\frac{\Phi(t)}{2}}{cos^2\frac{\Phi(t)}{2}}$$

$$= tan^2\frac{\Phi(t)}{2}$$

The phase difference between the modulating signals can be expressed as:

$$\Phi(t) = 2\ arctan\sqrt{\frac{P_{-1}}{P_1}} \quad (13)$$

Here, the frequency of modulating signal is defined as f_m, n describes the refractive index inside the RF cable, L represents the difference between RF path, the phase difference between the modulating signals can also be written in the form of

$$\Phi(t) = \frac{\frac{nL}{c}}{\frac{}{2\pi f_m}} = \frac{2\pi nL}{c}f_m \quad (14)$$

By combining Equation 13 and 14, the frequency of input modulating signal can be directly derived from the ratio of 1st and -1st order sideband power

$$f_m = \frac{c}{\pi nL}arctan\sqrt{\frac{P_{-1}}{P_1}} \quad (15)$$

3. Experimental setup and results

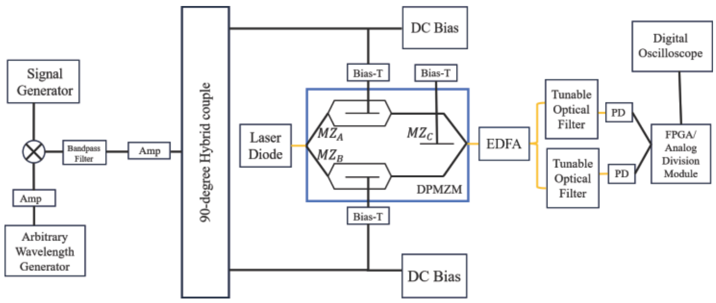

Figure 2. Experimental setup for frequency measurement using the optical SSB modulation

Fig. 2 illustrates the experimental setup. The output from a RF signal generator and the sweep signal generated by an arbitrary wave generator (AWG) were combined by a RF mixer. A 90-degree hybrid coupler was applied to induce the 90-degree phase difference between the modulating signal inserted to two sub MZMs. The DC bias voltages of the DPMZM were adjusted to realize SSB modulation. The optical outputs were amplified using an erbium-doped fiber amplifier (EDFA), and the output from the modulator was split into two paths. This configuration allows the measurement of the power of the 1st order sideband in one

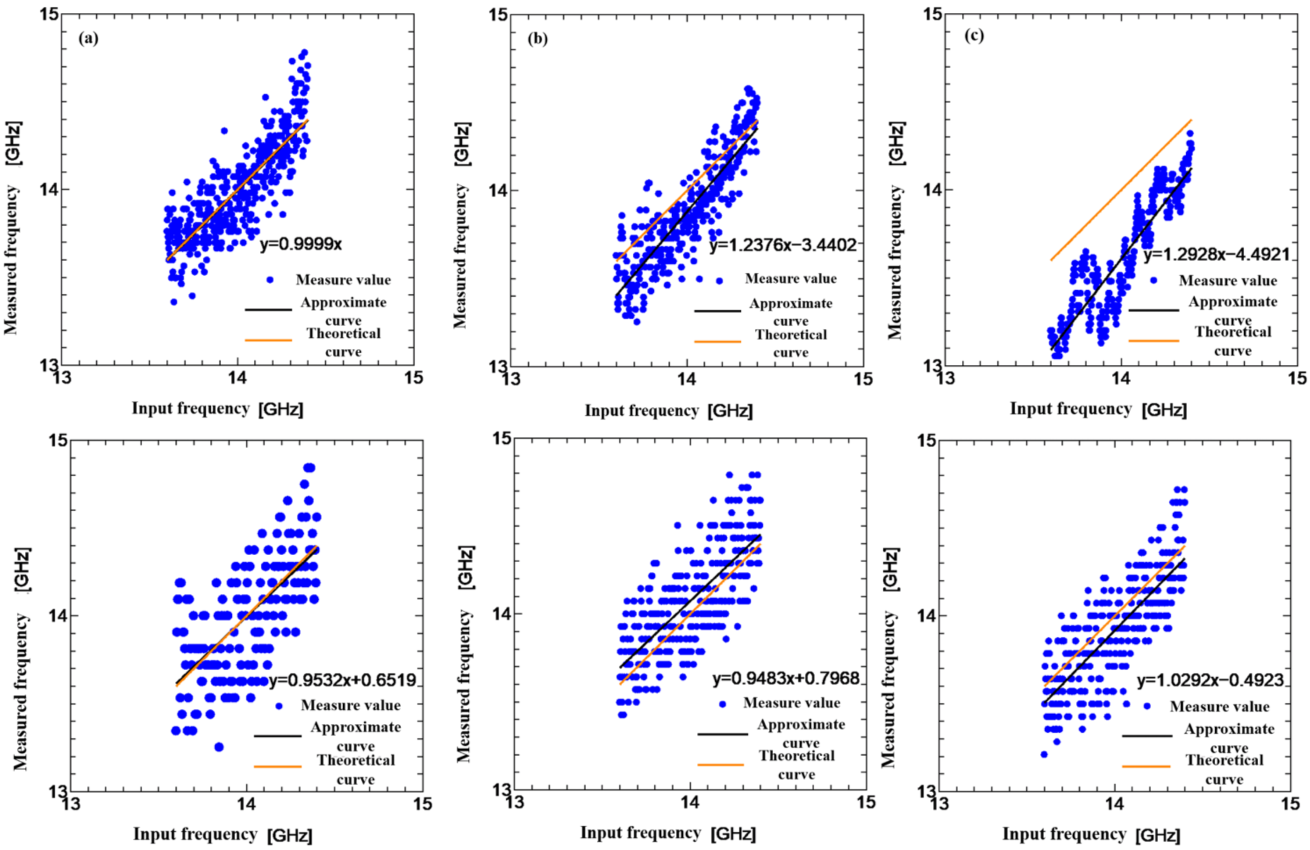

Figure 3. SSB modulation based frequency measurement results (a) results obtained by analog division module under 5ms sweep time (b) 1ms sweep time measurment results (analog division module) (c) 100µs sweep time measurment results (analog division module) (d) results obtained by FPGA under 5ms sweep time (e) 1ms sweep time measurment results (FPGA) (f) 100µs sweep time measurment results(FPGA)

path and that of the -1st order sideband in the other path. The optical filter has a minimum resolution of 0.1 nm, and the center wavelength was set to the wavelengths of the 1st order and -1st order sidebands when a 14 GHz signal was input to the modulator. The filtered optical signals are converted into electrical signals using photodetectors (PD) because optical spectrum analysis requires relatively longer sweep time. The ratio of P_{-1} to P_1 is calculated by the FPGA or the analog division module and the measurement result is shown using a digital oscilloscope.

One signal generator generates a signal with a frequency of 18 GHz while the other AWG generates a signal that that was swept from 3.5 to 4.5 GHz. As a result, a sweeping signal in the range of 13.5 GHz to 14.5 GHz was generated and input as the modulating signal. Measurements were conducted at three different sweep speeds: 5 ms, 1 ms, and 100 µs. Due to the characteristics of the optical filter, the sideband ratio measured by the oscilloscope exhibited errors as the frequency changed. However, since the optical filter characteristics remain constant regardless of sweep speed, the results were corrected using the 5 ms sweep time as a reference.

Table 1. Errors of SSB modulation-based frequency measurement

Sweep speed	5ms	10ms	100μs
Average relative errors (Analog division module)	0.86%	1.18%	2.81%
Maximum relative errors (Analog division module)	2.92%	4.09%	5.47%
Average relative errors (FPGA)	1.45%	1.30%	1.20%
Maximum relative errors (FPGA)	4.28%	4.24%	4.07%

The measurement errors are listed in Table 1. Fig. 3(a-c) show frequency measurement results when the analog division modules were applied. Fig. 3(d-f) show the FPGA processing results. For measurements using the analog division module, errors increased as the sweep time decreased. These results indicate that FPGA-based measurements exhibited higher overall errors, primarily because the analog division module operates at a bandwidth of 15 MHz, while the FPGA samples at 250 MHz. This higher sampling rate introduces noise over a wider bandwidth, reducing measurement accuracy. However, incorporating an RF filter can enhance the accuracy of FPGA-based measurements by suppressing unwanted noise.

4. Conclusion

An instantaneous frequency measurement method utilizing SSB modulation of a DPMZM, combined with FPGA and analog division module processing, was proposed. This technique enables real-time phase difference calculations. In the designed circuit, phase changes were directly proportional to frequency variations, making real-time frequency detection feasible. The method was experimentally demonstrated using both analog and digital processing units, with overall measurement errors remaining below 5%. The analog processing performance degraded at higher sweep speeds, while digital processing maintained consistent accuracy across different sweep speeds. Furthermore, FPGA-based measurements can be improved by integrating an RF filter to eliminate undesired noise. We believe that this this measurement technique will be beneficial for solving the radio interference of in-vehicle radar.

5. Acknowledgements

This paper includes research results from studies funded by Commissioned Research (JPJ012368C04901 and JPJ012368C06001) of the National Institute of Information and Communications Technology (NICT), Japan, and results from research supported by JSPS KAKENHI Grant Number JP22H05196. This study is also supported by Japan Science and Technology Agency (JST) as part of Adopting Sustainable Partnerships for Innovative Research Ecosystem (ASPIRE), Grant Number JPMJAP2324.

References

[1] S. Kar, P. Mishra and K. -C. Wang, "5G-IoT Architecture for Next Generation Smart Systems," 2021 IEEE 4th 5G World Forum (5GWF), Montreal, QC, Canada, 2021, pp. 241-246, doi: 10.1109/5GWF52925.2021.00049.

[2] K. Ikeda et al., "Transmission Experiment of IEEE 802.11ad under FMCW Radar Interference Environment in Vehicle," 2021 IEEE 94th Vehicular Technology Conference (VTC2021-Fall), Norman, OK, USA, 2021, pp. 1-4, doi: 10.1109/VTC2021-Fall52928.2021.9625299.

[3] T. Kawanishi, T. Sakamoto and M. Izutsu, "High-Speed Control of Lightwave Amplitude, Phase, and Frequency by Use of Electrooptic Effect," in IEEE Journal of Selected Topics in Quantum Electronics, vol. 13, no. 1, pp. 79-91, Jan.-Feb. 2007, doi: 10.1109/JSTQE.2006.889044.

[4] T. Kawanishi, Double Sideband and Single Sideband Modulation. In Electro-Optic Modulation for Photonic Networks: Precise and High-Speed Control of Lightwaves; Springer: Berlin/Heidelberg, Germany, 2022; pp. 169-195.

[5] T. Kawanishi, Precise Optical Modulation and Its Application to Optoelectronic Device Measurement. Photonics 2021, 8, 160. https://doi.org/10.3390/photonics8050160